

Sublimation of Snow

Jessica D. Lundquist[®], ^a Julie Vano, ^b Ethan Gutmann, ^c Daniel Hogan, ^a Eli Schwat, ^a Michael Haugeneder, ^d Emilio Mateo, ^b Steve Oncley, ^c Chris Roden, ^c Elise Osenga, ^b and Liz Carver^b

KEYWORDS:

Hydrometeorology; Radiation budgets; Snow cover; Stability; Sublimation; Surface fluxes **ABSTRACT**: Snow is a vital part of water resources, and sublimation may remove 10%–90% of snowfall from the system. To improve our understanding of the physics that govern sublimation rates, as well as how those rates might change with the climate, we deployed an array of four towers with over 100 instruments from NCAR's Integrated Surface Flux System from November 2022 to June 2023 in the East River watershed, Colorado, in conjunction with the U.S. Department of Energy's Surface Atmosphere Integrated Field Laboratory (SAIL) and the National Oceanic and Atmospheric Administration (NOAA)'s Study of Precipitation, the Lower Atmosphere and Surface for Hydrometeorology (SPLASH) campaigns. Mass balance observations, snow pits, particle flux sensors, and terrestrial lidar scans of the evolving snowfield demonstrated how blowing snow influences sublimation rates, which we quantified with latent heat fluxes measured by eddy-covariance systems at heights 1–20 m above the snow surface. Detailed temperature profiles at finer resolutions highlighted the role of the stable boundary layer. Four-stream radiometers indicated the important role of changing albedo in the energy balance and its relationship to water vapor losses. Collectively, these observations span scales from seconds to seasons, from boundary layer turbulence to valley circulation to mesoscale meteorology. We describe the field campaign, highlights in the observations, and outreach and education products we are creating to facilitate cross-disciplinary dialogue and convey relevant findings to those seeking to better understand Colorado River snow and streamflow.

SIGNIFICANCE STATEMENT: Snow provides over 80% of water for the overallocated Colorado River, and in recent years, less runoff has occurred per unit snowfall. Sublimation, the conversion of ice to water vapor, results in less water for runoff, but due to a historic lack of observations, this process is hard to constrain. Variations in how sublimation is represented in models have led to a large divergence of projected water resource availability for the Colorado River basin over both current and future climates. The field campaign described here provides the first comprehensive examination of how snow accumulates, blows around, evolves, and sublimates over 8 months in the Colorado Rocky Mountains, providing a critical benchmark for process understanding and model development.

DOI: 10.1175/BAMS-D-23-0191.1

Corresponding author: Jessica D. Lundquist, jdlund@uw.edu Supplemental information related to this paper is available at the Journals Online website: https://doi.org/10.1175/BAMS-D-23-0191.s1.

Manuscript received 21 July 2023, in final form 23 February 2024, accepted 12 March 2024

© 2024 American Meteorological Society. This published article is licensed under the terms of the default AMS reuse license. For information regarding reuse of this content and general copyright information, consult the AMS Copyright Policy (www.ametsoc.org/PUBSReuseLicenses).

AFFILIATIONS: ^a Civil and Environmental Engineering, University of Washington, Seattle, Washington; ^b Aspen Global Change Institute, Aspen, Colorado; ^c National Center for Atmospheric Research, Boulder, Colorado; ^d WSL Institute for Snow and Avalanche Research SLF, Davos Dorf, Switzerland

1. Introduction

In 2021, the Colorado River basin snowpack was 80% of average but only delivered around 30% of average flows. This is concerning for the 40 million people who depend on the river (Fleck and Udall 2021). Many are now asking, where did the snow water go? Is snow water likely to disappear like this again in the future? Snow is a vital part of water resources (Huss et al. 2017), but sublimation may remove 10%–90% of snowfall from the hydrologic system (Strasser et al. 2008). When atmospheric input is held constant, the largest uncertainty in modeling snow hydrology is sublimation (Slater et al. 2001; Xia et al. 2017). Due to a critical lack of reliable measurements of snow sublimation, we do not fully understand the physics that govern current rates of sublimation, let alone how those amounts might change with the climate. This adds uncertainty to our ability to understand current linkages between the atmosphere and land surface and hinders our ability to predict and manage water resources (Vano et al. 2014).

Most land surface models assume that sublimation and its corresponding latent heat flux obey Monin–Obukhov similarity theory and that bulk aerodynamic methods for calculating turbulent fluxes (Stull 1988) are approximately valid. Similarity theory requires stationary, horizontally homogenous boundary layers. However, the boundary layer over snow in complex terrain is likely to deviate from these conditions in multiple ways (Mahrt et al. 2018; Mott et al. 2018; Stiperski et al. 2019). In addition, turbulence may be intermittently generated above the stable boundary layer, leading to fluxes that vary with height and net downward transport of heat and momentum (Grachev et al. 2005). Atmospheric flow around complex terrain is regularly subject to wind shear and frequently generates wave-like structures that interact with the stable boundary layer. These lead to brief periods of intense mixing that are hard to measure and model (Helgason and Pomeroy 2012; Litt et al. 2017; Mortarini et al. 2018; Sun et al. 2015). Currently, no turbulence stability schemes in land surface models represent these events well (Lapo et al. 2019), and even further complexity arises when forests are present (Lundquist et al. 2021; Sexstone et al. 2018).

At higher wind speeds, blowing snow is common, with blowing snow observed during 50% of the winter at one Colorado alpine site (Berg 1986). Blowing snow processes and their contribution to sublimation are only included in a few snow models (e.g., Liston and Elder 2006; Pomeroy et al. 2007; Vionnet et al. 2014), and the process is not considered in large-scale land surface models. In cases of blowing snow, the surface roughness is hard to define, and much of the turbulent kinetic energy must go toward keeping the snow particles suspended, reducing the turbulent energy available for mixing (Bintanja 2000). Most conclusions about the role of blowing snow in sublimation are based on modeling, and results vary widely. Bintanja (2001) suggested that sublimation from blowing snow would saturate the layer, leading to water vapor feedbacks that dampen total sublimation. Vionnet et al. (2014) calculated that modeling sublimation from both the surface and blowing snow resulted in three times more sublimation than sublimation from the surface alone. Mott et al. (2018) reviewed

blowing snow loss estimates in 13 papers and found disagreements in the impact of blowing snow on the snowpack, ranging from a 0.1% seasonal loss up to a 41% seasonal loss. While some differences were due to differences in weather conditions across sites, many differences arose from model complexity and parameterizations.

Eddy-covariance systems have been deployed over snow with some success (Reba et al. 2009, 2012). However, outside of a few field campaigns, e.g., Fluxes over Snow Surfaces II (FLOSSII) (Mahrt and Vickers 2005), Snow-Horizontal Array Turbulence Study (SnoHATS) (Bou-Zeid et al. 2010), and Surface Heat Budget of the Arctic Ocean (SHEBA) (Grachev et al. 2005), studies of turbulent fluxes over snow have been limited to one or two sonic anemometers. These can give high-quality results when placed within traditional boundary layer conditions (Bou-Zeid et al. 2010, 2007), but as discussed above, both stable and blowing snow conditions lead to fluxes that vary with height above the surface. Thus, it remains unclear how representative isolated measurements are in complex terrain (Helgason and Pomeroy 2012; Litt et al. 2017; Stiperski and Rotach 2016), in stable conditions (Lapo et al. 2019), and in cases of blowing snow (Aksamit and Pomeroy 2018; Sigmund et al. 2022). Given the expense and maintenance required, it also remains unclear what is the best approach to measuring snow sublimation at watershed scales.

To investigate these issues, we deployed the Earth Observing Laboratory (EOL)'s Integrated Surface Flux System (ISFS) in partnership with the U.S. Department of Energy (DOE)'s Surface Atmosphere Integrated Field Laboratory (SAIL) (Feldman et al. 2023) and the National Oceanic and Atmospheric Administration (NOAA)'s Study of Precipitation, the Lower Atmosphere and Surface for Hydrometeorology (SPLASH) (de Boer et al. 2023) campaign in the East River watershed (Fig. 1) to bring together observations essential to span scales from seconds to seasons, from turbulence to valley-circulation to mesoscale meteorology, to constrain this difficult and societally relevant problem.

2. Background: What do we know about sublimation?

Sublimation, the direct transfer of frozen water to the vapor phase, is a thermodynamics problem: it occurs because snow crystals are made of water molecules, which, statistically, will leave the snow in some number (just like the evaporation of water at any temperature). At the same time, water molecules in the form of water vapor will condense onto the snow in some number. Thus, the magnitude and direction of sublimation rates scale with the vapor pressure gradient between the snow surface and the air above. In a closed system without any wind or exchange of air, sublimation would eventually cease because the water vapor pressure in the air would reach saturation/equilibrium and the water vapor pressure gradient would approach zero.

Thus, sublimation is a turbulence problem. Because the atmosphere is not a closed system, at least on the scales we care about, the movement of air above the snow surface determines how rapidly and efficiently water vapor is moved away from the snow surface, such that a water vapor pressure gradient is maintained and sublimation can continue.

Sublimation impacts both the mass and energy balance of the snow surface, where we track the mass balance through snow water equivalent (SWE), and we track the surface energy balance through the snow surface temperature $T_{\rm ss}$. The main contributors to the snow mass balance are

$$\frac{\partial SWE}{\partial t} = snowfall - sublimation - melt + redistribution.$$
 (1)

Sublimation leaves a signal in the change in snow water equivalent ($\partial SWE/\partial t$) most clearly at times with no snowfall or melt but may peak simultaneously with times of major snow redistribution (blowing snow).

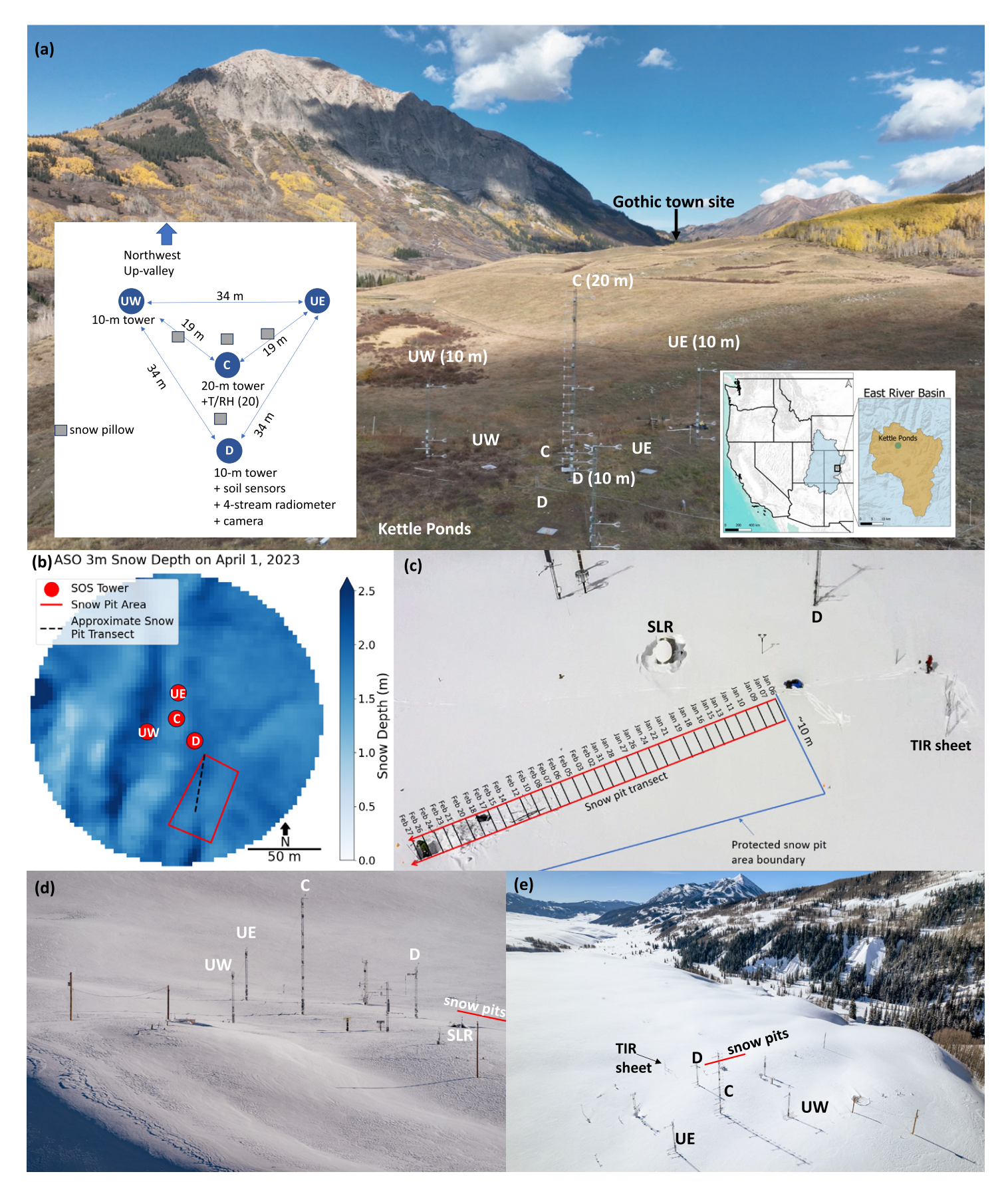


Fig. 1. (a) Location and setup of the SOS field campaign at Kettle Ponds, Gothic, Colorado, looking upvalley. (b) Snow depth distribution at and around the site, as measured by the Airborne Snow Observatory (Painter et al. 2016) on 1 Apr 2023. (c) Locations of snow pits from 6 Jan through 27 Feb, in relation to the D tower, the SPLASH snow level radar (SLR), and the thermal infrared (TIR) sheet setup. Arrows indicate locations of snow pits dug later in the season. (d),(e) Views of site on 23 Mar 2023, with (d) showing snow drifts in relation to towers and (e) looking down-valley.

Changes in the snow surface temperature $(\partial T_{SS}/\partial t)$ reflect the net fluxes of the energy balance:

$$c_{p}^{SS} \frac{\partial T_{SS}}{\partial t} = LW_{in} - \varepsilon \sigma T_{SS}^{4} + (1 - \alpha)SW_{in} - \lambda \frac{\partial T_{S}}{\partial z} - LH - SH + E_{melt},$$
 (2)

where λ is the thermal conductivity of snow, ε is the emissivity (\sim 0.99 for snow), $c_p^{\rm SS}$ is the specific heat of snow, and α is the snow albedo. Fluxes include melt ($E_{\rm melt}$), incoming longwave radiation (LW $_{\rm in}$), incoming shortwave radiation (SW $_{\rm in}$), conduction into the snowpack [λ (∂T_s / ∂z)], and sensible heat flux SH, in addition to latent heat flux (LH). At standard atmospheric pressure and 0°C, the latent heat of sublimation of ice L_s is 2835 J g⁻¹, the sum of the heat required for melt L_m (334 J g⁻¹) and for evaporation (2501 J g⁻¹). Thus, the influence of sublimation on the energy balance is large, and the mass and energy components of sublimation can be related to each other.

3. Site and setup: The Sublimation of Snow (SOS) field campaign

The study focuses on the snow and air space at Kettle Ponds (39.07°N, 107.07°W, 2861 m), about 2 km downvalley from the Rocky Mountain Biological Laboratory (RMBL), Gothic, Colorado, coincident with the SAIL and SPLASH field campaigns (de Boer et al. 2023; Feldman et al. 2023). The site is in an open location, with the surface experiencing primarily along-valley winds, with a long fetch (>1 km) over snow without large obstructions. Historic wind measurements indicate that the site is calm 43% of the time, with the strongest sustained winds reaching $10-12\,\mathrm{m}\,\mathrm{s}^{-1}$ from the northwest (NW) direction. Thus, it experiences both stable conditions and winds high enough to suspend snow to heights above 2 m (Gossart et al. 2017). The location is slightly raised from the valley's river bottom. Valley walls are offset from the site by about 0.8 km on either side, with slopes of 36%. The site is far enough away from trees and buildings to focus on the study questions of snow and mountain winds without added complexity.

The main SOS deployment took place from 1 November 2022 to 18 June 2023 and consisted of four towers, each with a corresponding snow pillow, arranged in a triangle at Kettle Ponds (Fig. 1, Table 1 in the online supplemental material). The center tower (C) is 20 m in height, to provide a link to intermittent turbulent mixing originating from above the boundary layer, and the surrounding three towers are each 10 m in height, bounding a triangular control volume and monitoring horizontal heterogeneity. Pairs of sonic anemometers and open-path gas analyzers were deployed on the center tower at heights of 1, 2, 3, 5, 10, 15, and 20 m and on the outer towers at heights of 1, 3, and 10 m. Terrestrial laser scanners (TLSs), two mounted on each outer tower, scanned a 70° 3D cone every 5 min, measuring snow heights, blowing snow characteristics, and how these changed through time. Hygrothermometers measured temperature and relative humidity every meter on the central tower, and a mobile "thermistor harp" with thermistors spaced 0.5 cm apart was manually placed on the snow surface on some clear nights.

To quantify the mass balance [Eq. (1)], fluidless snow pillows (Heggli et al. 2018) were installed within the triangular control volume and within the footprint of the eddy-covariance sensors to measure snow water equivalent and its change through time. During the winter intensive observing period, two white boxes, following Stössel et al. (2010), were manually inserted into the snow, flushed with the snow surface, and weighed to measure snow losses to (sublimation) and gained from (condensation) the atmosphere. Manual snow pits (Fig. 1) were taken almost every day from January to mid-March to provide reference profiles of snow temperature, density, and crystal sizes.

To quantify the energy balance [Eq. (2), supplemental Table 1], two four-component radiometers measured the radiative heat flux, including the surface albedo. Soil temperature

sensors were distributed between 32 cm below the soil to the surface, and thermistors were arranged every 10 cm from 0.4 to 1.2 m above ground. These sensors measured temperature profiles and heat exchange within the snowpack for the winter period up until snow melted around the sensors. A heat flux plate at the base of the downwind (D) tower documented ground—snow heat exchange. Four fast-response (0.2 s) infrared (IR) sensors (Apogee SIF-111) documented the snow surface temperature and its changes related to both turbulence fluctuations and longer time scales. A Jenoptik VarioCAM HiRes thermal IR camera recorded videos of a thin synthetic sheet (2 m high and 3 m wide) deployed vertically adjacent to the snow surface (Fig. 8). The surface temperature of the sheet serves as a proxy for the local air temperature. The collected data illustrate variability in surface temperatures (Haugeneder et al. 2023; Lundquist et al. 2018).

To quantify blowing snow, in particular the saltating layer, we installed two FlowCapt sensors over the lowest 2 m of the upwind-east (UE) 10-m tower. These measure the acoustic signal of particle impacts over the vertical extent of the sensor tube and have reliable performance quantifying particle flux during nonprecipitating events (Trouvilliez et al. 2015).

4. Highlights of winter 2022/23

a. Evolving surface: Snow accumulation, redistribution, and melt. We tracked weather patterns in a weekly weather blog describing where storms originated from and how they presented themselves in the East River basin. Most storms in 2022/23 were associated with particularly active atmospheric river systems that first impacted California, and the remnants of these storms delivered regular moisture to the southern Rocky Mountains. While the first snow fell just days after the site was installed in late October, snow cover remained thin and patchy until late November (Fig. 2). Snow depth exceeded half a meter for the first time in late December, with the first of a sequence of near-weekly snowstorms, illustrated by rapid increases in snow depth that continued through mid-January. Storms became less frequent in February and then delivered substantially more moisture in March (Fig. 2a). Snow pit locations moved through time (Fig. 1c), with a measured drop in SWE and depth in early February (Fig. 2a), when pit observations progressed from a drift to locations with shallower snow (Fig. 1b). Snow pit densities were regularly about 5% denser than density derived from depth and weight on the snow pillows. This may be due to consistent measurement bias or to natural spatial variability.

Sublimation rates, measured as vertical water vapor flux (Fig. 2c), were generally small, with larger values on 22 December, the date of strongest winds (Fig. 2e), and in the spring during snowmelt, particularly when snow cover became patchy (Fig. 2a). The cumulative sum of vertical water vapor flux, as measured by the center tower 3-m sensor, came to $44 \, \text{kg m}^{-2}$ on 20 May (Fig. 2c), which is the equivalent of 0.04 m, about 10% of the season's maximum snow accumulation (0.44 m SWE at the D and UE pillows). Temperatures remained below freezing most of the winter (Fig. 2d), with warmer temperatures in April corresponding to increases in snow density (Fig. 2b) and snowmelt (Fig. 2a).

b. Moving surface: Blowing snow and a changing landscape. Our combined measurements provide a unique perspective on both how blowing snow shapes the ground surface of the winter landscape and how water vapor fluxes are influenced by the presence of blowing snow. On 22 December, average hourly 20-m winds exceeding 17 m s⁻¹ (Fig. 2e), associated with a strong upper-level jet from the northwest, moved snow from landscape ridges into landscape depressions. These changes were recorded by variable snow depth and snow water equivalent, where simultaneous increases and decreases were observed across the study site (Fig. 3). Repeat captures of the snow surface from the scanning lidar (Fig. 3) illustrated snow movement from locally raised areas to fill in longitudinally contiguous depressions. Of the four snow pillows, only the UW pillow was located in a filling area.

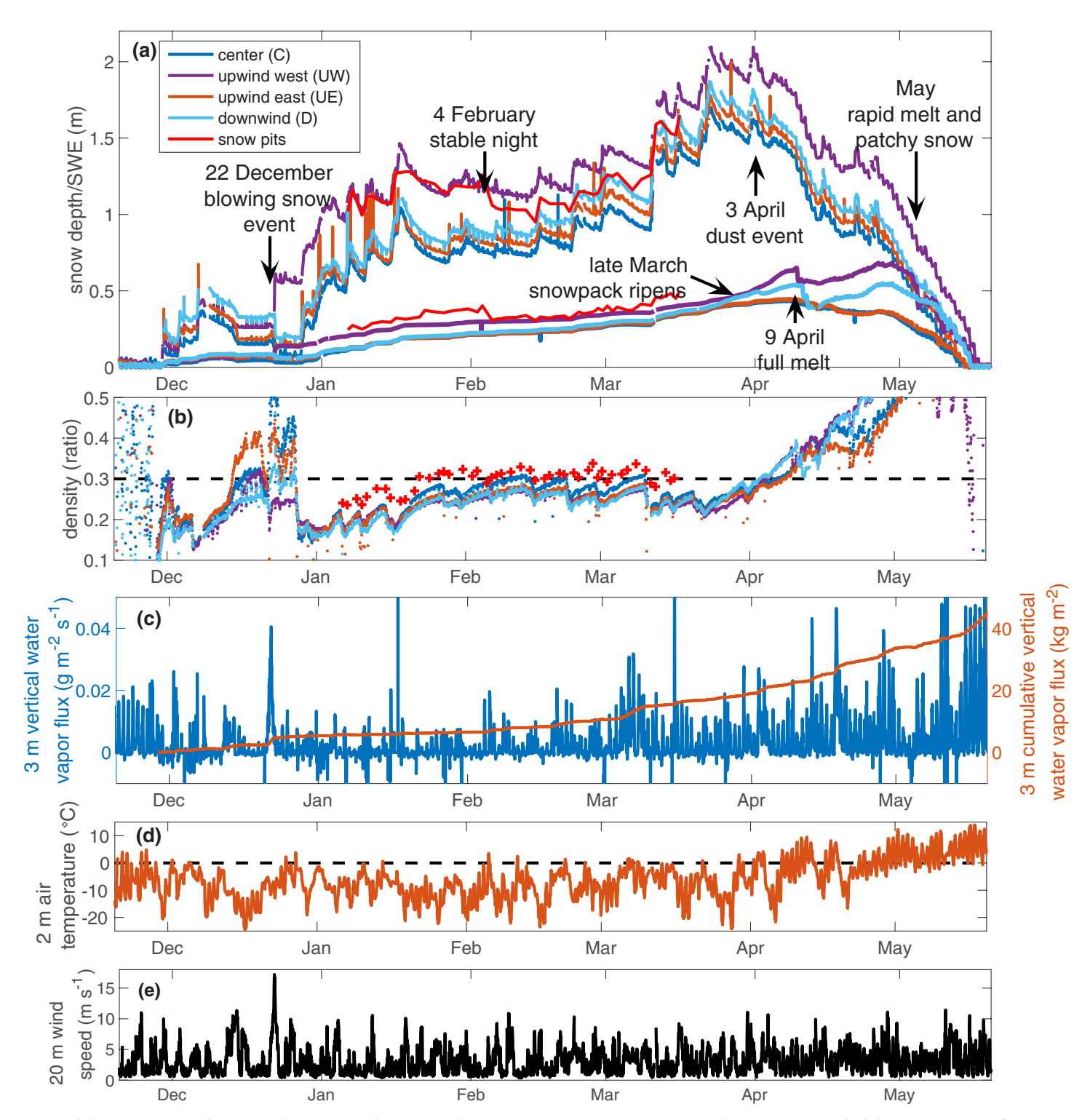


Fig. 2. (a) Snow depth (thin lines) and SWE (thick lines) at the pillow and pit locations (shown in Fig. 1), (b) snow density [derived from SWE/depth from (a)], (c) time series and cumulative vertical water vapor flux at 3 m (center tower), (d) air temperature (2 m height, center tower), and (e) mean wind speed (20-m height, center tower). All values are hourly averages. Significant events, discussed further below, are marked in (a).

The eddy-covariance systems (Fig. 3c) observed the highest sublimation rates coincident with the time of greatest snow relocation and also demonstrated variable rates of sublimation with elevation above the surface. However, more a detailed analysis is required to interpret this vertical flux divergence because blowing snow creates measurement difficulties for open-path sensors. Eddy-covariance measurements during this event had the lowest counts of successful instantaneous 20-Hz measurements per 5-min average of the season, with 80% of 5-min averages having at least 10% missing and 29% of 5-min averages having more than

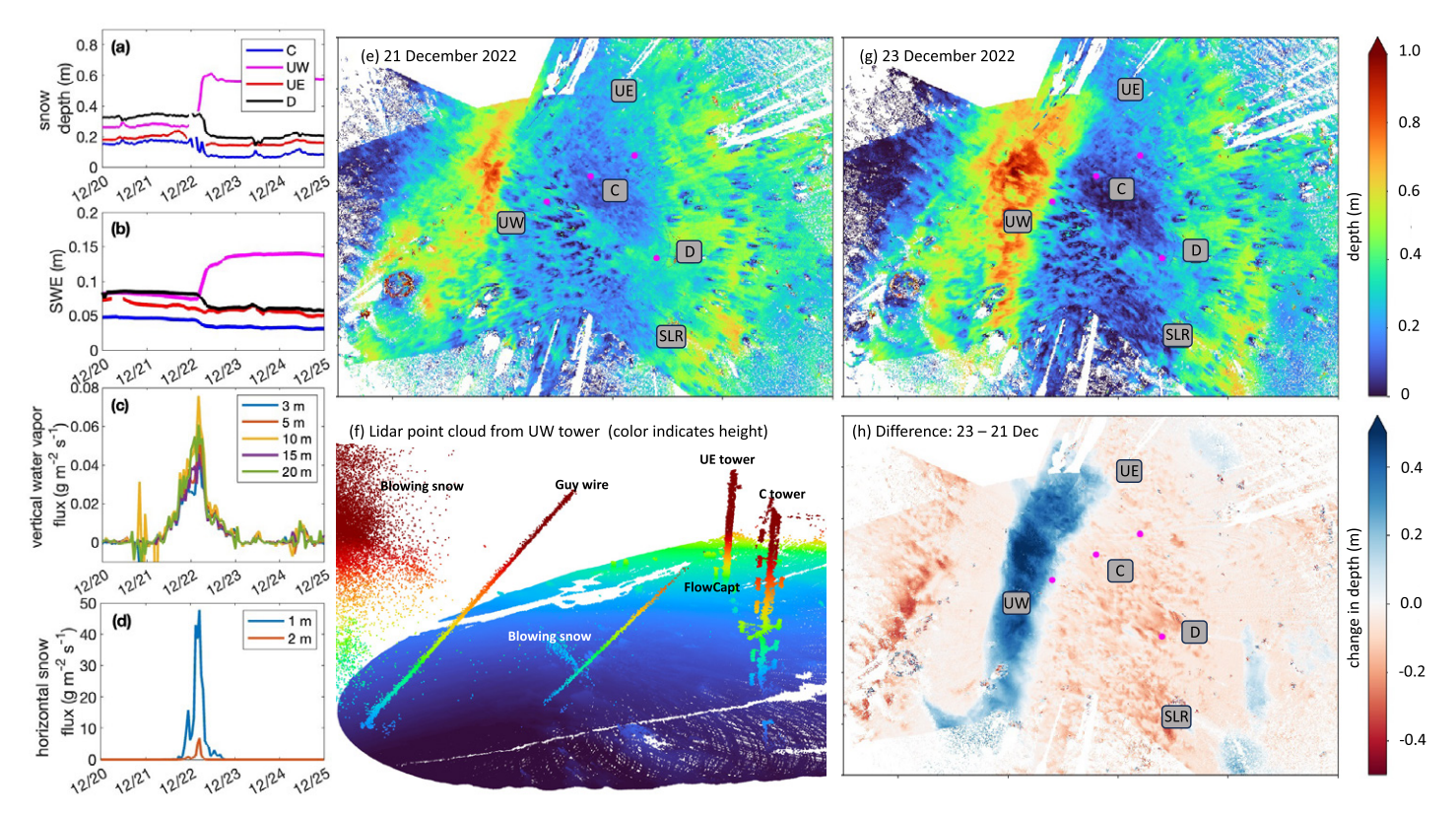


Fig. 3. (a) Snow depth, averaged over the footprint of each snow pillow (~1 m²), from the lidars, (b) SWE, (c) vertical water vapor flux from the eddy-covariance sensors on the central tower, and (d) horizontal snow particle flux from the FlowCapt on the upper-east tower. Lidar-derived snow depths on (e) 21 Dec and (g) 23 Dec, with (h) the change between them. Rectangles indicate the four tower locations and the SLR, and pink dots indicate snow pillow locations. Small-scale variations highlight drifts near bushes. (f) Illustration of lidar point cloud, including blowing snow, towers, and surface elevations.

50% missing. The 1-m sonics were buried during this event, leading to 100% loss of data. The FlowCapt sensors (Fig. 3d) recorded hourly average maximum horizontal snow particle flux rates of $48 \, \mathrm{g} \, \mathrm{m}^{-2} \, \mathrm{s}^{-1}$ at the lower sensor and $7 \, \mathrm{g} \, \mathrm{m}^{-2} \, \mathrm{s}^{-1}$ at the higher sensor.

c. Separate surface: Inversions, insulation, and turbulence decoupling. The stable boundary layer above the snow surface was observed through vertical arrays of temperature sensors at increasingly fine resolutions near the snow surface (Fig. 4). At all scales, during stable conditions, the greatest rate of change in temperature is nearest the surface, in the lowest meter, centimeter, and millimeter. Temperature profiles extending through the snowpack at the D and UW towers matched well with each other and with manual snow pit measurements so long as they were adjusted to reflect distance from the snow surface, which was frequently the coldest point in the profile throughout the winter (Fig. 5). This suggests that any horizontal variation in temperature was small compared to the vertical variation.

Subsurface arrays of temperature sensors (Fig. 5) observed soils freezing in the fall, with the lowest soil temperatures near the soil surface. After snow accumulated to greater than 20-cm depth (mid-December), the snow insulated the soil, such that soil temperatures no longer fluctuated diurnally, and the soils warmed from below. Cold air temperatures from December to mid-March (Fig. 2d) kept the snow surface well below freezing. The snowpack warmed substantially after 15 March, cooled again during some late March storms, and then warmed again in early April, reaching isothermal conditions near 0°C on 9 April, described more below.

d. Darkening surface: Dust on snow and the radiative energy balance. A snowstorm 3–4 April 2023 brought significant dust from Arizona to the field site. Initially buried under

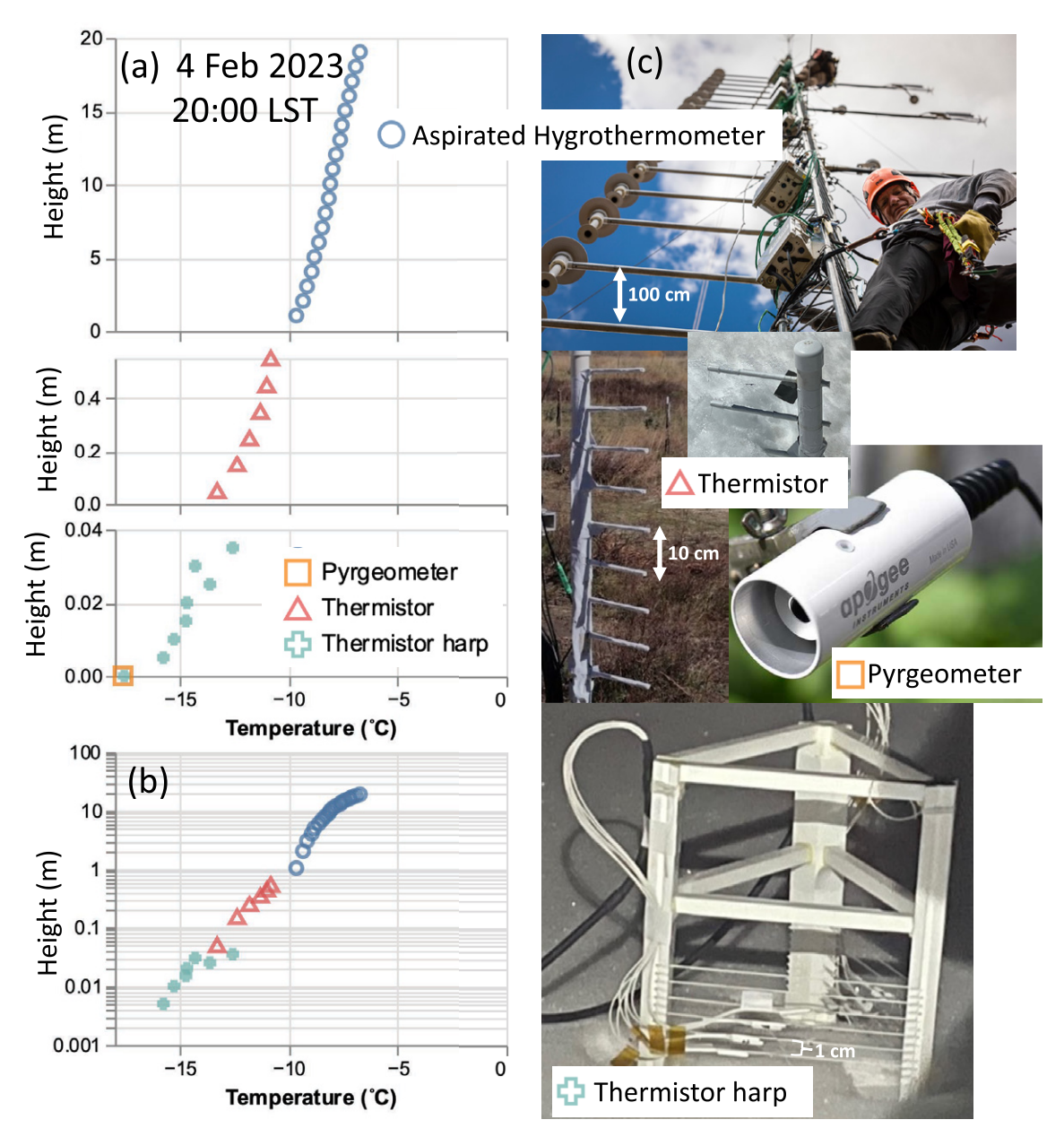


Fig. 4. Nocturnal inversion at 2000 LST 4 Feb 2023 measured at three different scales at various heights above the snow surface, from (a) the temperature/humidity sensors on the center tower, spaced 100 cm apart; the thermistor array, spaced 10 cm apart, with only sensors above the snow plotted here; the thermistor harp, with thermistors spaced 1 cm apart on two faces, offset to achieve 0.5-cm vertical resolution, placed on the snow on clear nights such that the lowest thermistor touched the snow surface; and the Apogee thermal IR pyrgeometer, which observes the snow surface temperature, assuming an emissivity of 0.98. (b) As in (a), but combined on a log scale. (c) Photos of all the instruments. The harp was located near the Gothic town site; all other measurements were at Kettle Ponds as indicated in Fig. 1.

a few centimeters of new snow, the dust became exposed (visible in both camera imagery and albedo observations) starting 7 April, becoming darker in the days following. Around this time, snow began to melt (see snow becoming isothermal in Fig. 5 and soil moisture increasing in Fig. 7). The decrease in snow albedo, defined as the ratio of outgoing to incoming radiation, associated with this dust exposure was over 20% (Fig. 6c). In photographs, meltwater moving along the top of the snow appeared to concentrate the dust in certain locations (Figs. 6d–f), and the peak hourly net radiation available for melt increased by about $200 \,\mathrm{W}\,\mathrm{m}^{-2}$ (Fig. 6a). Dust remained visible on the snow for the rest of the melt season (Fig. 6). This period of greater net radiative energy (Fig. 6a) corresponded to increased vertical water

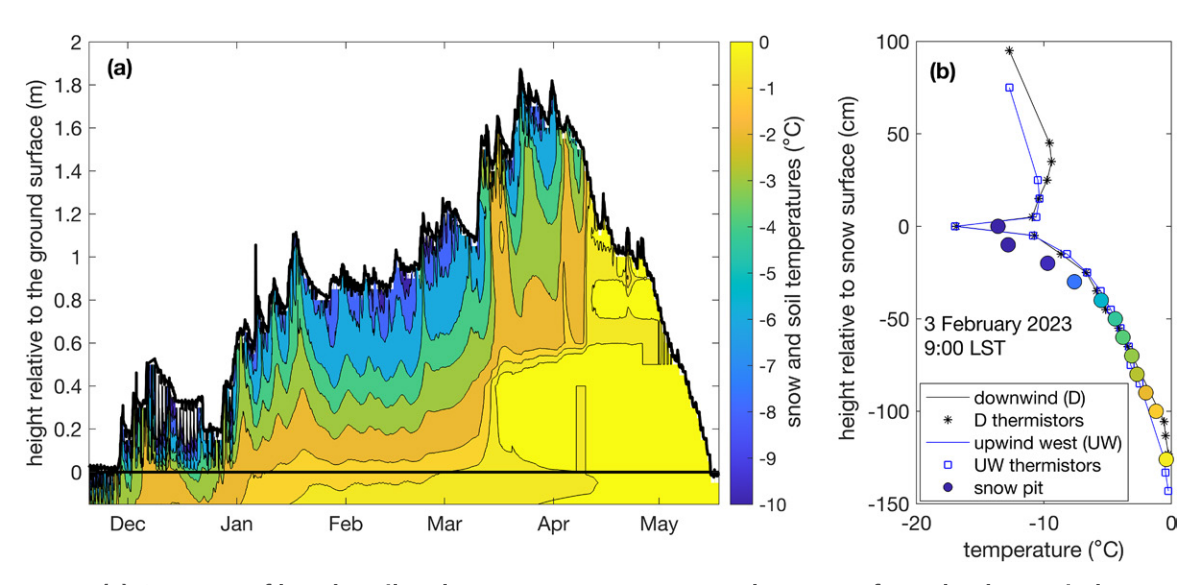


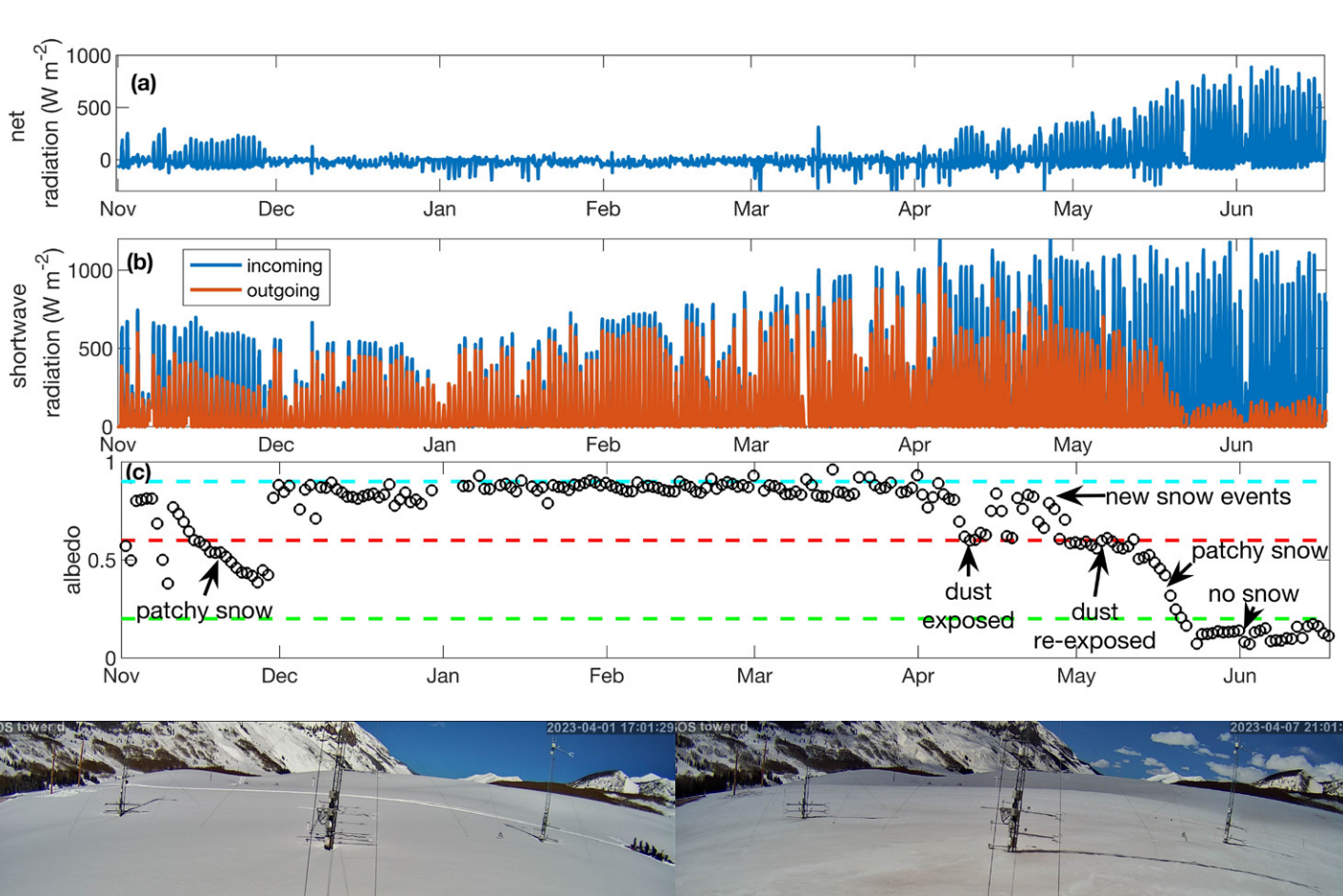
Fig. 5. (a) Contours of hourly soil and snow temperatures over the season from the downwind tower thermistor array. Thick black lines indicate ground surface and snow surface (as detected by lidar, for the downwind pillow location). Sensors began breaking during the spring melt, so contour distinctions between -1° and 0°C in mid-April and later are less reliable. (b) Comparison of snow pit temperature profile with thermistor profiles and radiometric surface temperatures (assuming an emissivity of 0.98) from the UW and D towers on 3 Feb 2023. Snow pit temperatures are colored to match the contour plot.

vapor flux (Fig. 2c). Thus, the increased energy available led to both melt and sublimation, although at this point, the eddy-covariance system could also be measuring evaporation of meltwater from the snow surface.

e. *Melting surface: Moving water and the mass and energy balance.* The beginning of April was a period of rapid warming of the snowpack (Fig. 5). At this point in the season, the total radiative energy balance was positive during the day and negative at night (Fig. 6a). We hypothesize that the changes in SWE observed across the snow pillows at this time (Fig. 7a), which occurred simultaneously with decreases in snow depth (Fig. 2a), were associated with spatial variations in surface melt and meltwater flowpaths. Due to most of the snowpack being below freezing in early April (Fig. 5), we hypothesize that this meltwater flowed through the snowpack and refroze, resulting in increasing SWE at the UW and D snow pillows (Fig. 7a) at the same time snow depth was decreasing and no SWE changes were measured at the C and UE snow pillows. During this period, the temperatures at the majority of the thermistors in the snowpack were below 0°C (Fig. 5). The meltwater reached the bottom of the snowpack right after 9 April, as evidenced by a rapid increase in soil moisture (Fig. 7b), a warming of the coldest near-surface soil layer temperature (Fig. 7c), a spike in the soil heat flux (Fig. 7d), and likely, a rapid decrease in the weight of the pooled water in the snowpack, as evidenced by a decline in SWE at the UW and D sites (Fig. 7a).

5. Outreach and education

Because sublimation spans the scientific fields of atmospheric science and snow science, parts of the process are generally confusing to any discipline specialist and are hard to find in general education curricula. To illuminate the science of sublimation to students, disciplinary scientists, and the general public, we developed outreach material throughout the project. In addition to several short videos currently under development, we established an instrument library (Fig. 8), with photos and short video clips explaining what each instrument in the project looks like and is used for. The clips were used extensively in a graduate-level snow hydrology class, where class laboratories are primarily based on the data presented here, which



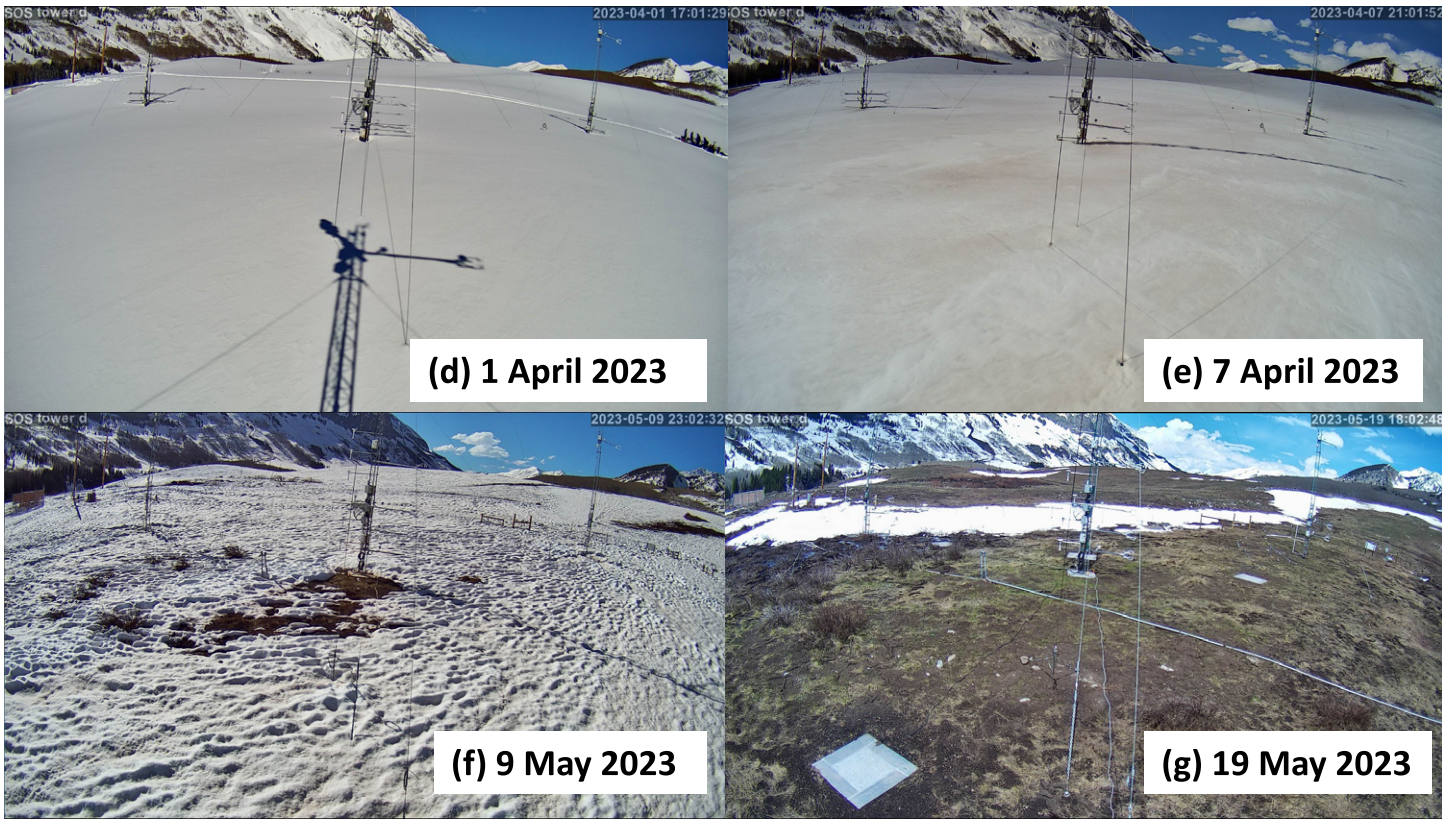


Fig. 6. (a) Hourly net radiation, incoming minus outgoing longwave and shortwave, primarily measured at the D tower, which had a higher quality sensor, but patched with data from the UW tower radiometer from 11 to 23 May, (b) incoming and outgoing shortwave radiation from (a), and (c) albedo, calculated at the time of peak incoming solar radiation each day. Horizontal dashed lines indicate typical albedo values for new snow (0.9), dirty snow (0.6), and bare ground (0.2). (d)–(g) Photos of the field site through the spring melt season. The snow remaining on 19 May corresponds to the drift location visible in Fig. 1 and highlighted in Fig. 3.

teaches graduate students from any discipline about the snow mass and energy balance using Python notebooks and analysis of the SOS dataset. Many of the graphs presented within this paper were developed in conjunction with assignments from this class, as students and researchers worked together to understand the snow at Kettle Ponds.

6. Conclusions and directions for future work

The unique combination of instruments from the SOS field campaign illuminated a number of snow and boundary layer science phenomena. The combination of multiple, vertically stacked sonic anemometers with blowing snow flux sensors allowed us to observe the role of blowing snow in increasing sublimation rates and the occurrence of vertical divergence in latent heat fluxes that appears to accompany the suspension of snow. The largest vertical latent heat flux measured prior to the snowmelt season occurred during the December wind event (Figs. 2 and 3). The combination of FlowCapt and lidar sensors demonstrated how extreme seasonal wind events can redistribute snow across the landscape, in some locations increasing snow depth by nearly 100% (Fig. 3). Our measurements also allowed us to characterize the stability of the atmospheric boundary layer. High-resolution vertical temperature profile measurements at nested scales indicated that extremely steep positive temperature gradients (in some cases, nearly 5°C change over 2 cm) occurred frequently through the winter snow season. Finally, we observed the strong effects of dust deposition on snow surface albedo and snowmelt.

Project partners at DOE and NOAA are focusing on improving their land surface, Earth system, and weather forecast models. Observations collected through

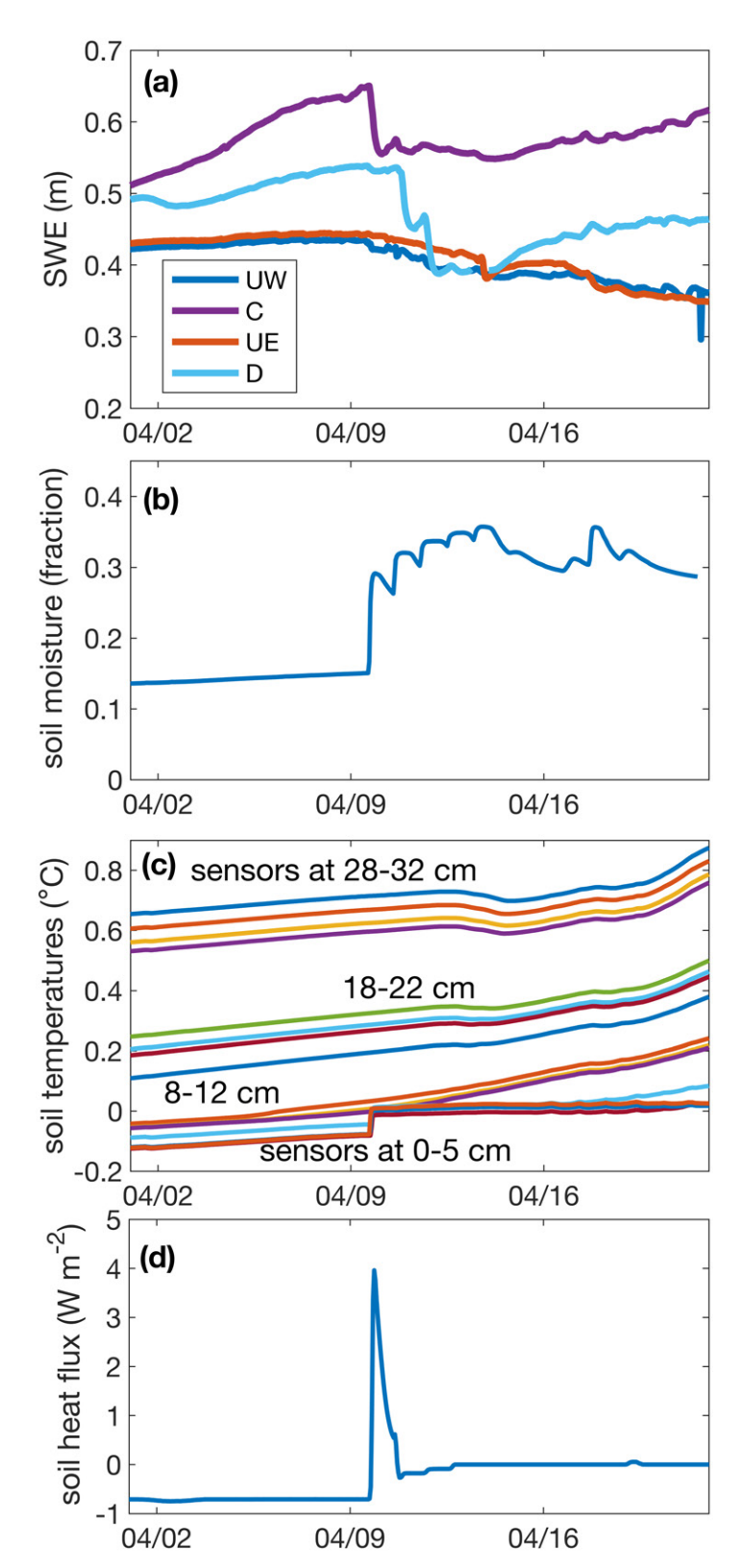


Fig. 7. Snowmelt began in early April and reached the soil on 9 Apr, as evidenced by (a) SWE, (b) soil moisture, (c) soil temperature, and (d) soil heat flux.

this work include all variables associated with the snow energy balance and will be ideal for benchmarking surface fluxes over snow in mountains to test the myriad parameterizations of snow processes contained in these models. Observations collected through the SOS campaign will also serve future efforts by evaluating what approaches are sufficient for producing

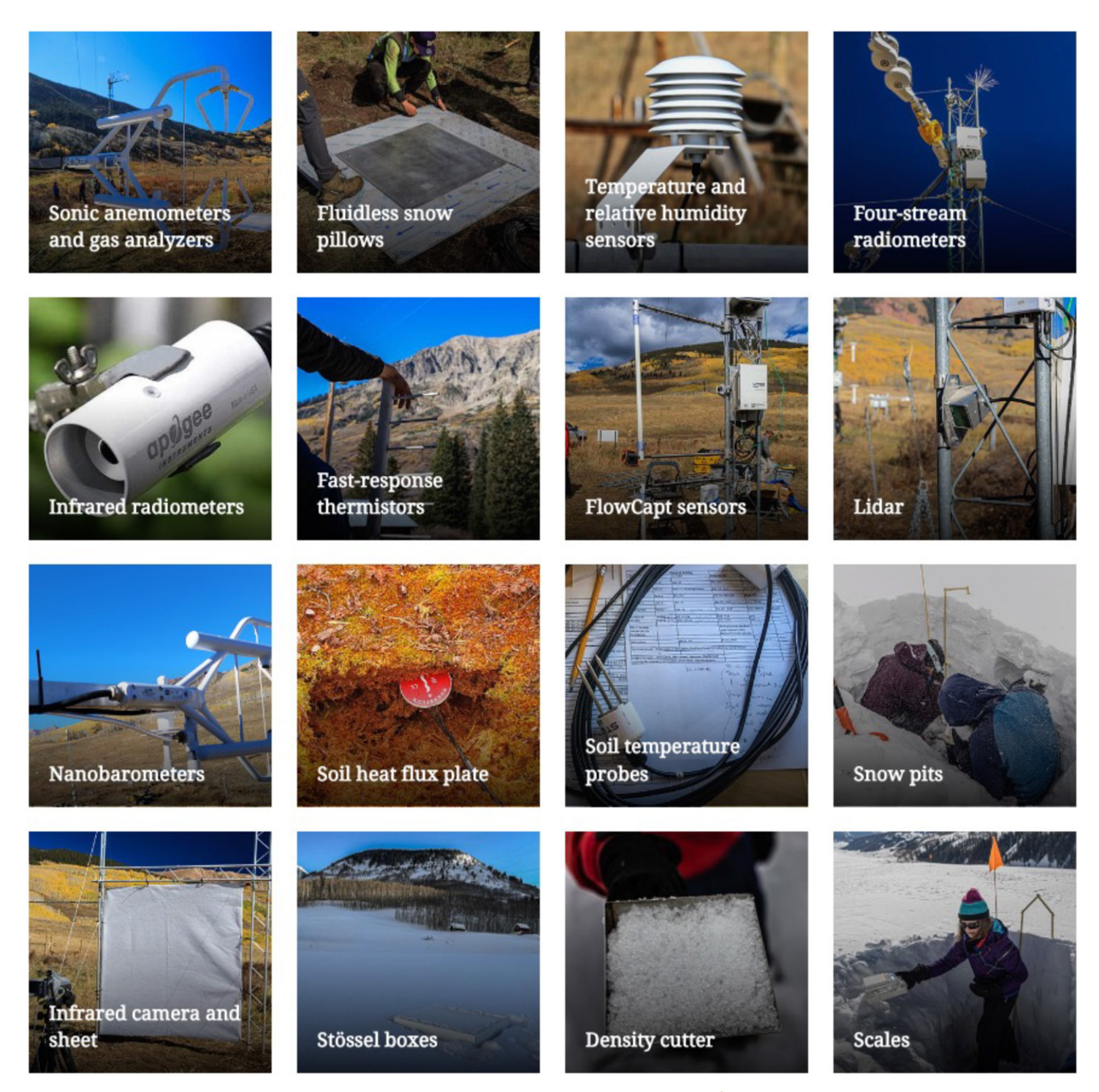


Fig. 8. The SOS Instrument Library, available at https://www.agci.org/sublimation-of-snow.

unbiased estimates of snow sublimation, which are critical for both seasonal and longer-term water resources prediction and management.

Acknowledgments. We thank the Rocky Mountain Biological Laboratory, particularly Jennifer Reithel, Eric Hulm, Ian Breckheimer, and billy barr, for their help in facilitating the field setup and data collection. We thank the entire NCAR EOL team, including Antonio Vigil, William Nicewonger, Tony Wiese, David Ortigoza, Gary Granger, Jacquelyn Witte, Matthew Paulus, Linda Echo-Hawk, and Isabel Suhr, for their excellence in all things related to data collection. We thank Daniel Feldman and Gijs de Boer for their collaboration with the SAIL and SPLASH campaigns, respectively. For site

photography, we thank Mark Stone (Fig. 1a) from the University of Washington and Jeremy Snyder (Figs. 1d,e) from the University of California Berkeley. We thank Tim Shcherbina and Anthony Shcherbina for help with field installation. We thank Matthew Sturm and Andrey Shcherbina for advice on designing the fine-scale temperature measurements. This work was supported by National Science Foundation Awards 2139836 and 2139809. M. Haugeneder received funding from SNF (Swiss National Science Foundation) Grant 188554.

Data availability statement. SOS data (NSF-NCAR/EOL-ISFS-Team 2023) can be accessed from the SOS Project Page at NCAR: https://data.eol.ucar.edu/project/SOS. The data report can also be found under Documentation on the page: https://data.eol.ucar.edu/dataset/633.001. These locations will also be where any further-revised final datasets will be archived. Example processing code and lab assignments can be found at the University of Washington Snow Hydrology class website and associated GitHub repository: https://mountain-hydrology-research-group.github.io/snow-hydrology/.

References

- Aksamit, N. O., and J. W. Pomeroy, 2018: The effect of coherent structures in the atmospheric surface layer on blowing-snow transport. *Bound.-Layer Meteor.*, **167**, 211–233, https://doi.org/10.1007/s10546-017-0318-2.
- Berg, N. H., 1986: Blowing snow at a Colorado alpine site: Measurements and implications. *Arct. Alp. Res.*, **18**, 147–161. https://doi.org/10.2307/1551124
- Bintanja, R., 2000: Snowdrift suspension and atmospheric turbulence. Part I: Theoretical background and model description. *Bound.-Layer Meteor.*, 95, 343–368, https://doi.org/10.1023/A:1002676804487.
- —, 2001: Modelling snowdrift sublimation and its effect on the moisture budget of the atmospheric boundary layer. *Tellus*, **53A**, 215–232, https://doi.org/10.3402/tellusa.v53i2.12189.
- Bou-Zeid, E., M. B. Parlange, and C. Meneveau, 2007: On the parameterization of surface roughness at regional scales. *J. Atmos. Sci.*, **64**, 216–227, https://doi.org/10.1175/JAS3826.1.
- —, C. Higgins, H. Huwald, C. Meneveau, and M. B. Parlange, 2010: Field study of the dynamics and modelling of subgrid-scale turbulence in a stable atmospheric surface layer over a glacier. *J. Fluid Mech.*, 665, 480–515, https://doi.org/10.1017/S0022112010004015.
- de Boer, G., and Coauthors, 2023: Supporting advancement in weather and water prediction in the upper Colorado River basin: The SPLASH campaign. Bull. Amer. Meteor. Soc., 104, E1853—E1874, https://doi.org/10.1175/BAMS-D-22-0147.1.
- Feldman, D. R., and Coauthors, 2023: The Surface Atmosphere Integrated Field Laboratory (SAIL) campaign. *Bull. Amer. Meteor. Soc.*, **104**, E2192–E2222, https://doi.org/10.1175/BAMS-D-22-0049.1.
- Fleck, J., and B. Udall, 2021: Managing Colorado River risk. *Science*, **372**, 885, https://doi.org/10.1126/science.abj5498.
- Gossart, A., and Coauthors, 2017: Blowing snow detection from ground-based ceilometers: Application to East Antarctica. *Cryosphere*, **11**, 2755–2772, https://doi.org/10.5194/tc-11-2755-2017.
- Grachev, A. A., C. W. Fairall, P. O. G. Persson, E. L. Andreas, and P. S. Guest, 2005: Stable boundary-layer scaling regimes: The Sheba data. *Bound.-Layer Meteor.*, 116, 201–235, https://doi.org/10.1007/s10546-004-2729-0.
- Haugeneder, M., M. Lehning, D. Reynolds, T. Jonas, and R. Mott, 2023: A novel method to quantify near-surface boundary-layer dynamics at ultra-high spatiotemporal resolution. *Bound.-Layer Meteor.*, 186, 177–197, https://doi.org/10. 1007/s10546-022-00752-3.
- Heggli, A., M. Heggli, and T. Trauman, 2018: Research and development in advancing fluidless snow water content monitoring. 86th Annual Western Snow Conf., Albuquerque, NM, Western Snow Conference, https://westernsnowconference.org/bibliography/2018Heggli.pdf.
- Helgason, W., and J. W. Pomeroy, 2012: Characteristics of the near-surface boundary layer within a mountain valley during winter. *J. Appl. Meteor. Climatol.*, **51**, 583–597, https://doi.org/10.1175/JAMC-D-11-058.1.
- Huss, M., and Coauthors, 2017: Toward mountains without permanent snow and ice. *Earth's Future*, **5**, 418–435, https://doi.org/10.1002/2016EF000514.
- Lapo, K., B. Nijssen, and J. D. Lundquist, 2019: Evaluation of turbulence stability schemes of land models for stable conditions. J. Geophys. Res. Atmos., 124, 3072–3089, https://doi.org/10.1029/2018JD028970.
- Liston, G. E., and K. Elder, 2006: A distributed snow-evolution modeling system (SnowModel). *J. Hydrometeor.*, **7**, 1259–1276, https://doi.org/10.1175/JHM548.1.
- Litt, M., J.-E. Sicart, D. Six, P. Wagnon, and W. D. Helgason, 2017: Surface-layer turbulence, energy balance and links to atmospheric circulations over a mountain glacier in the French Alps. *Cryosphere*, **11**, 971–987, https://doi.org/10.5194/tc-11-971-2017.
- Lundquist, J. D., C. Chickadel, N. Cristea, W. R. Currier, B. Henn, E. Keenan, and J. Dozier, 2018: Separating snow and forest temperatures with thermal infrared remote sensing. *Remote Sens. Environ.*, 209, 764–779, https://doi.org/10. 1016/j.rse.2018.03.001.

- —, S. Dickerson-Lange, E. Gutmann, T. Jonas, C. Lumbrazo, and D. Reynolds, 2021: Snow interception modelling: Isolated observations have led to many land surface models lacking appropriate temperature sensitivities. *Hydrol. Processes*, 35, e14274, https://doi.org/10.1002/hyp.14274.
- Mahrt, L., and D. Vickers, 2005: Moisture fluxes over snow with and without protruding vegetation. *Quart. J. Roy. Meteor. Soc.*, 131, 1251–1270, https://doi.org/10.1256/qj.04.66.
- —, C. K. Thomas, A. A. Grachev, and P. O. G. Persson, 2018: Near-surface vertical flux divergence in the stable boundary layer. *Bound.-Layer Meteor.*, 169, 373–393, https://doi.org/10.1007/s10546-018-0379-x.
- Mortarini, L., D. Cava, U. Giostra, O. Acevedo, L. G. Nogueira Martins, P. E. Soares de Oliveira, and D. Anfossi, 2018: Observations of submeso motions and intermittent turbulent mixing across a low level jet with a 132-m tower. *Quart. J. Roy. Meteor. Soc.*, **144**, 172–183, https://doi.org/10.1002/qj.3192.
- Mott, R., V. Vionnet, and T. Grünewald, 2018: The seasonal snow cover dynamics: Review on wind-driven coupling processes. *Front. Earth Sci.*, **6**, 197, https://doi.org/10.3389/feart.2018.00197.
- NSF-NCAR/EOL-ISFS-Team, 2023: SOS: ISFS surface meteorology and flux products. Version 1.0, accessed 11 February 2024, https://doi.org/10.26023/CYK2-SR3N-880J.
- Painter, T. H., and Coauthors, 2016: The Airborne Snow Observatory: Fusion of scanning lidar, imaging spectrometer, and physically-based modeling for mapping snow water equivalent and snow albedo. *Remote Sens. Environ.*, **184**, 139–152, https://doi.org/10.1016/j.rse.2016.06.018.
- Pomeroy, J. W., D. M. Gray, T. Brown, N. R. Hedstrom, W. L. Quinton, R. J. Granger, and S. K. Carey, 2007: The cold regions hydrological model: A platform for basing process representation and model structure on physical evidence. *Hydrol. Processes*, 21, 2650–2667, https://doi.org/10.1002/hyp.6787.
- Reba, M. L., T. E. Link, D. Marks, and J. Pomeroy, 2009: An assessment of corrections for eddy covariance measured turbulent fluxes over snow in mountain environments. *Water Resour. Res.*, 45, W00D38, https://doi.org/10.1029/ 2008WR007045.
- —, J. Pomeroy, D. Marks, and T. E. Link, 2012: Estimating surface sublimation losses from snowpacks in a mountain catchment using eddy covariance and turbulent transfer calculations. *Hydrol. Processes*, 26, 3699–3711, https://doi.org/10.1002/hyp.8372.
- Sexstone, G. A., D. W. Clow, S. R. Fassnacht, G. E. Liston, C. A. Hiemstra, J. F. Knowles, and C. A. Penn, 2018: Snow sublimation in mountain environments and its sensitivity to forest disturbance and climate warming. *Water Resour. Res.*, 54, 1191–1211, https://doi.org/10.1002/2017WR021172.
- Sigmund, A., and Coauthors, 2022: Evidence of strong flux underestimation by bulk parametrizations during drifting and blowing snow. *Bound.-Layer Meteor.*, **182**, 119–146, https://doi.org/10.1007/s10546-021-00653-x.
- Slater, A. G., and Coauthors, 2001: The representation of snow in land surface schemes: Results from PILPS 2(d). *J. Hydrometeor.*, **2**, 7–25, https://doi.org/10.1175/1525-7541(2001)002<0007:TROSIL>2.0.CO;2.
- Stiperski, I., and M. W. Rotach, 2016: On the measurement of turbulence over complex mountainous terrain. *Bound.-Layer Meteor.*, **159**, 97–121, https://doi.org/10.1007/s10546-015-0103-z.
- ——, M. Calaf, and M. W. Rotach, 2019: Scaling, anisotropy, and complexity in near-surface atmospheric turbulence. J. Geophys. Res. Atmos., 124, 1428– 1448, https://doi.org/10.1029/2018JD029383.
- Stössel, F., M. Guala, C. Fierz, C. Manes, and M. Lehning, 2010: Micrometeorological and morphological observations of surface hoar dynamics on a mountain snow cover. Water Resour. Res., 46, W04511, https://doi.org/10. 1029/2009WR008198.
- Strasser, U., M. Bernhardt, M. Weber, G. E. Liston, and W. Mauser, 2008: Is snow sublimation important in the alpine water balance? *Cryosphere*, **2**, 53–66, https://doi.org/10.5194/tc-2-53-2008.
- Stull, R. B., 1988: An Introduction To Boundary Layer Meteorology. Kluwer, 666 pp.

- Sun, J., and Coauthors, 2015: Review of wave-turbulence interactions in the stable atmospheric boundary layer. *Rev. Geophys.*, **53**, 956–993, https://doi.org/10. 1002/2015RG000487.
- Trouvilliez, A., F. Naaim-Bouvet, H. Bellot, C. Genthon, and H. Gallée, 2015: Evaluation of the FlowCapt acoustic sensor for the aeolian transport of snow. *J. Atmos. Oceanic Technol.*, **32**, 1630–1641, https://doi.org/10.1175/JTECH-D-14-00104.1.
- Vano, J. A., and Coauthors, 2014: Understanding uncertainties in future Colorado River streamflow. *Bull. Amer. Meteor. Soc.*, **95**, 59–78, https://doi.org/10.1175/BAMS-D-12-00228.1.
- Vionnet, V., E. Martin, V. Masson, G. Guyomarc'h, F. Naaim-Bouvet, A. Prokop, Y. Durand, and C. Lac, 2014: Simulation of wind-induced snow transport and sublimation in alpine terrain using a fully coupled snowpack/atmosphere model. *Cryosphere*, 8, 395–415, https://doi.org/10.5194/tc-8-395-2014.
- Xia, Y., D. Mocko, M. Huang, B. Li, M. Rodell, K. E. Mitchell, X. Cai, and M. B. Ek, 2017: Comparison and assessment of three advanced land surface models in simulating terrestrial water storage components over the United States. J. Hydrometeor., 18, 625–649, https://doi.org/10.1175/JHM-D-16-0112.1.